THEORY AND APPLICATION OF THE IN-CORE NEUTRON NOISE INDUCED BY FLUCTUATING CORE BOUNDARIES

Vasiliy Arzhanov[*] and Imre Pázsit
Department of Reactor Physics, Chalmers University of Technology,
Gibraltargatan 3, SE - 412 96 Göteborg, Sweden
arj@nephy.chalmers.se; imre@nephy.chalmers.se

ABSTRACT

The paper develops a general theory of the neutron noise induced by fluctuating boundaries. First, a simple one-group model of a homogeneous reactor is considered to derive the solution in the frequency domain through the Green's function technique. In addition, linear reactor kinetics is defined for systems with varying size. Second, the paper extends the one-group homogeneous analysis to the general multi-group non-homogeneous model. The full solution in the frequency domain is given through the Green's function of the unperturbed system, the static flux, and a quantity describing the boundary movements. A multi-group absorber model is proposed to represent the oscillating boundary. The model turns out to be very useful, for instance, to derive the point reactor and adiabatic approximations of the neutron noise arising from the fluctuating boundary. Third, the paper gives an equivalent solution in terms of the adjoint function. This is important for certain practical problems because in energy dependent cases, such as the multi-group approximation, the adjoint function approach has certain advantages over the Green's function method. Finally, the paper applies the general solution for a cylindrical model of a pressurized water reactor (PWR) to investigate the in-core neutron noise induced by fluctuating core boundaries.

1. INTRODUCTION

This work presents development of the theory on space-time dependence of the in-core neutron flux (neutron noise) induced by oscillating core boundaries. This topic has received some new interest recently, initially in connection with the investigation on the neutron noise induced by the vibration of control rods [1]. Description of such a perturbation requires the treatment of moving boundaries or interfaces. In addition, there exist other cases of practical problems where the treatment of a moving boundary is necessary. Enrichment/reprocessing plants are one example, because a solution of fissile material at the plants is contained in a tank with a free surface. Material flow into and out from the tank will change the surface position. Even a perturbation of the free surface without volume change (travelling or standing waves) may occur. Besides the space-time dependent flux variations, even simpler quantities, such as the time dependence of the reactivity, are of vital importance. Another example is the future accelerator driven subcritical systems (ADS) for which a molten salt type construction is one potential candidate. In such a reactor again a free surface of a liquid core is conceivable. Finally, as the most important practical application in current pressurized water reactors, various types of core-barrel vibrations are known to occur. Out of these the so-called shell-mode vibrations are a typical case of a system with a varying shape, i.e. with a fluctuating boundary. Core-

[*]Permanent address: Keldysh Institute of Applied Mathematics, 125047 Moscow, Russia

barrel vibrations have been diagnosed so far through the ex-core neutron noise, which is induced by the varying water thickness between the outer core surface and the pressure vessel [2]. However, the fluctuation of the boundary will also induce in-core noise in the case of shell-mode vibrations.

For the treatment of small variations (vibrations) of the boundary, there are several methods available, which are all equivalent: a time-dependent extrapolation length at the static boundary, the assumption of a time-varying absorbing layer at the static boundary, and the recently developed method of coordinate transformations [1, 3]. The equivalence of these methods was first proven for the simpler case of a slab reactor with one fixed and one varying boundary [1], then for the more complicated case of a vibrating absorber rod [3]. In addition, the point kinetic and adiabatic perturbations were also developed and investigated in [1] and [3]. The purpose of the present work is to develop a theoretical basis to treat this kind of problems in a much more general model than in the previous works, and demonstrate some applications.

2. ONE-GROUP HOMOGENEOUS MODEL

We start by assuming a homogeneous critical reactor, which at rest occupies a volume V_0. We have for the static flux in the one-group diffusion approximation

$$\begin{cases} D\nabla^2\phi_0(\mathbf{r}) + (\nu\Sigma_f - \Sigma_a)\phi_0(\mathbf{r}) = 0 \\ \beta\nu\Sigma_f\phi_0(\mathbf{r}) - \lambda C_0(\mathbf{r}) = 0 \end{cases} \tag{1}$$

Here all the symbols have their usual meaning. It is shown in [4] that the boundary condition of no incoming current is most appropriate in the case of moving boundaries. This leads to the concept of the extrapolation length for the boundary condition given on the static surface $S_0 = \partial V_0$ by

$$\left.\frac{\partial\phi_0(\mathbf{r})}{\partial n}\right|_{\mathbf{r}_B} = -\frac{1}{l}\phi_0(\mathbf{r}_B) \tag{2}$$

Here $\mathbf{r}_B$ is a variable point running over the static boundary S_0 and n is an outward normal on the boundary. The space- and time-dependent neutron flux and the precursor density obey the time-dependent one-group diffusion equations

$$\begin{cases} \dfrac{1}{\mathrm{v}}\dfrac{\partial\phi(\mathbf{r},t)}{\partial t} = D\nabla^2\phi(\mathbf{r},t) + \left[(1-\beta)\nu\Sigma_f - \Sigma_a\right]\phi(\mathbf{r},t) + \lambda C(\mathbf{r},t) \\ \dfrac{\partial C(\mathbf{r},t)}{\partial t} = \beta\nu\Sigma_f\phi(\mathbf{r},t) - \lambda C(\mathbf{r},t) \end{cases} \tag{3}$$

together with the boundary condition given at the momentary boundary S_M:

$$\left.\frac{\partial\phi(\mathbf{r},t)}{\partial n}\right|_{\mathbf{r}_M} = -\frac{1}{l}\phi\left(\mathbf{r}_M,t\right) \tag{4}$$

Figure 1 gives a visual explanation of the notation and defines the displacement $\varepsilon(\mathbf{r}_B,t)$ of the momentary boundary relative to the static one.

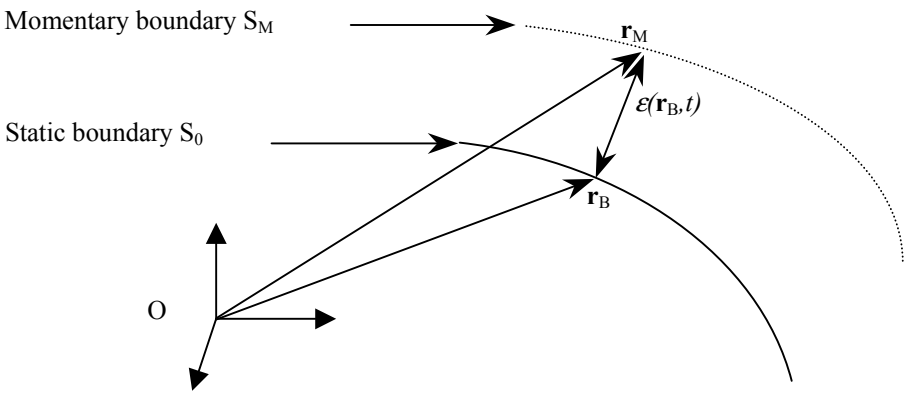

Figure 1. Displacement of the momentary boundary

Because $\phi(\mathbf{r},t)$ and $\phi_0(\mathbf{r})$ are defined over different spatial regions, we run into an immediate difficulty when we try to define the point reactor approximation as usual by postulating the relationship $\phi(\mathbf{r},t) = P(t)\phi_0(\mathbf{r})$. To alleviate this difficulty, it is convenient to introduce a boundary condition on the static surface S_0 such that it becomes an approximate version of the exact condition

$$\left.\frac{\partial\phi(\mathbf{r},t)}{\partial n}\right|_{\mathbf{r}_B} \approx -\frac{1}{l+\varepsilon(\mathbf{r}_B,t)}\phi\left(\mathbf{r}_B,t\right) \approx -\frac{1}{l}\phi\left(\mathbf{r}_B,t\right)+\frac{1}{l^2}\phi\left(\mathbf{r}_B,t\right)\varepsilon\left(\mathbf{r}_B,t\right) \tag{5}$$

Paper [4] discusses in detail a derivation of this boundary condition, which is equivalent to the case of a fixed boundary with a time-varying extrapolation length of $l(\mathbf{r}_B,t) = l + \varepsilon(\mathbf{r}_B,t)$. Having fixed the boundary condition one can use the traditional linearisation technique to derive linear frequency-dependent equations for systems with fluctuating boundaries. We decompose time-dependent quantities into a stationary component and a small deviation, put the decomposition into the original system (3) and the boundary condition (5), subtract the static equation, neglect second order terms, and finally Fourier transform the resulting equation. This yields in the end

$$\begin{cases} \nabla^2\delta\phi(\mathbf{r},\omega)+B^2(\omega)\delta\phi(\mathbf{r},\omega)=0 \\ \left.\dfrac{\partial\delta\phi(\mathbf{r},\omega)}{\partial n}\right|_{\mathbf{r}_B} = -\dfrac{1}{l}\delta\phi\left(\mathbf{r}_B,\omega\right)+\dfrac{1}{l^2}\phi_0\left(\mathbf{r}_B\right)\varepsilon\left(\mathbf{r}_B,\omega\right) \end{cases} \tag{6}$$

Here $B^2(\omega)$ is the frequency-dependent buckling defined through the zero reactor transfer function:

$$B^2(\omega) = B_0^2\left(1-\frac{1}{\rho_\infty G_0(\omega)}\right); \quad B_0^2=\frac{\nu\Sigma_f-\Sigma_a}{D}; \quad G_0(\omega)=\frac{1}{i\omega\left(\Lambda+\dfrac{\beta}{i\omega+\lambda}\right)} \tag{7}$$

The solution to problem (6) can be given through the Green's function belonging to the static problem, it is defined as

$$\begin{cases} \nabla_{\mathbf{r}}^2 G(\mathbf{r},\mathbf{r}',\omega)+B^2(\omega)G(\mathbf{r},\mathbf{r}',\omega)=\dfrac{1}{D}\delta(\mathbf{r}-\mathbf{r}') \\ \left.\dfrac{\partial G(\mathbf{r},\mathbf{r}',\omega)}{\partial n}\right|_{\mathbf{r}=\mathbf{r}_B} = -\dfrac{1}{l}G\left(\mathbf{r}_B,\mathbf{r}',\omega\right) \end{cases} \tag{8}$$

One way of deriving the solution is to multiply (8) by $\delta\phi$ and (6) by G, then subtract the two equations from each other and integrate over the static volume. Formally it goes as follows

$$\begin{aligned} \delta\phi(\mathbf{r},\omega)\times \quad & \frac{1}{D}\delta(\mathbf{r}-\mathbf{r}') = \nabla_{\mathbf{r}}^2 G(\mathbf{r},\mathbf{r}',\omega) + B^2(\omega)G(\mathbf{r},\mathbf{r}',\omega) \\ -G(\mathbf{r},\mathbf{r}',\omega)\times \quad & 0 = \nabla^2\delta\phi(\mathbf{r},\omega) + B^2(\omega)\delta\phi(\mathbf{r},\omega) \\ \hline = \int_{V_0} \delta\phi(\mathbf{r},\omega)\frac{1}{D}\delta(\mathbf{r}-\mathbf{r}')dV(\mathbf{r}) &= \int_{V_0}\left(\delta\phi\cdot\nabla_{\mathbf{r}}^2 G - G\cdot\nabla^2\delta\phi\right)dV(\mathbf{r}) \end{aligned} \tag{9}$$

Applying the Green's formula we have

$$\frac{1}{D}\delta\phi(\mathbf{r}',\omega) = \int_{\partial V_0}\left[\delta\phi(\mathbf{r}_B,\omega)\left.\frac{\partial G(\mathbf{r},\mathbf{r}',\omega)}{\partial n}\right|_{\mathbf{r}=\mathbf{r}_B} - G(\mathbf{r}_B,\mathbf{r}',\omega)\left.\frac{\partial\delta\phi(\mathbf{r},\omega)}{\partial n}\right|_{\mathbf{r}=\mathbf{r}_B}\right]dS(\mathbf{r}_B) \tag{10}$$

Taking into account the boundary conditions we derive finally

$$\delta\phi(\mathbf{r},\omega) = -\int_{\partial V_0} G(\mathbf{r},\mathbf{r}_B,\omega)\frac{1}{l^2}D\,\varepsilon(\mathbf{r}_B,\omega)\phi_0(\mathbf{r}_B)\,dS(\mathbf{r}_B) \tag{11}$$

Here the symmetry property of the Green's function has been used.

It is common to start theoretical studies on neutron noise by introducing a small variation in the absorption cross section, $\Sigma_a \to \Sigma_a + \delta\Sigma_a(\mathbf{r},t)$. The solution in the frequency domain is then given by linear perturbation theory as

$$\delta\phi(\mathbf{r},\omega) = \int_{V_0} G(\mathbf{r},\mathbf{r}',\omega)\,\delta\Sigma_a(\mathbf{r}',\omega)\,\phi_0(\mathbf{r}')\,dV(\mathbf{r}') \tag{12}$$

One can easily reduce (12) to (11) by defining the fluctuating part of the absorption cross-section as

$$\delta\Sigma_a(\mathbf{r},t) = -\frac{1}{l^2}D\,\varepsilon(\mathbf{r},t)\,\delta\left(f(\mathbf{r})-c\right) \tag{13}$$

Here we suppose a certain function $f(\mathbf{r})$ define the static boundary ∂V_0 by $f(\mathbf{r}) = c$. This is the absorber model, which treats the vibrating boundary as an infinitely thin absorbing layer (13).

Let us assume we study reactor kinetics by introducing the factorization $\phi(\mathbf{r},t) = P(t)\psi(\mathbf{r},t)$. Then one usually derives the point reactor equations and in particular the following relationship between the reactivity and the shape function [5]

$$\rho(t) = -\frac{\int_{V_0}\psi(\mathbf{r},t)\,\delta\Sigma_a(\mathbf{r},t)\,\phi_0(\mathbf{r})\,dV(\mathbf{r})}{\nu\Sigma_f\int_{V_0}\phi_0^2(\mathbf{r})dV} \tag{14}$$

The absorber model readily gives a general representation of the reactivity caused by the boundary fluctuations through the boundary displacement and the shape function

$$\rho(t) = \frac{\int_{\partial V_0}\psi(\mathbf{r}_B,t)\frac{1}{l^2}D\,\phi_0(\mathbf{r}_B)\,\varepsilon(\mathbf{r}_B,t)dS(\mathbf{r}_B)}{\nu\Sigma_f\int_{V_0}\phi_0^2(\mathbf{r})dV} \tag{15}$$

This immediately leads to different approximations of the reactivity term by assuming the point kinetic behavior, $\psi(\mathbf{r},t) = \phi_0(\mathbf{r})$, or the adiabatic behavior, $\psi(\mathbf{r},t) = \psi_{\mathrm{ad}}(\mathbf{r},t)$.

3. MULTI-GROUP NON-HOMOGENEOUS MODEL [6]

3.1 STATIC EQUATIONS

The steady-state model for an inhomogeneous system in the multi-group diffusion approximation, that generalizes the one-group model (1), reads as

$$\begin{cases} \nabla \cdot D^g \nabla \phi_{0,g} - \Sigma_a^g \phi_{0,g} + \sum_{g'} \Sigma_s^{g' \to g} \phi_{0,g'} + \chi^g \sum_{g'} \nu \Sigma_f^{g'} \phi_{0,g'} = 0 & g = 1, \ldots, N \\ \beta_j \sum_{g'} \nu \Sigma_f^{g'} \phi_{0,g'} - \lambda_j C_{0,j} = 0 & j = 1, \ldots, M \end{cases} \tag{16}$$

Here all the symbols have their usual meaning. The static fluxes together with the static precursor densities as well as the group cross-sections are space-dependent. The boundary condition of no incoming current in every group is defined through the group extrapolation length, l_g, as follows

$$\left. \frac{\partial \phi_{0,g}(\mathbf{r})}{\partial n} \right|_{\mathbf{r}_B} = -\frac{1}{l_g} \phi_{0,g}(\mathbf{r}_B) \tag{17}$$

3.1 DYNAMIC EQUATIONS

In the general case of the diffusion approximation, the space- and time-dependent neutron flux and the precursor density obey the time-dependent multi-group equations

$$\begin{cases} \frac{1}{\mathrm{v}_g} \frac{\partial \phi_g(\mathbf{r},t)}{\partial t} = \nabla \cdot D^g \nabla \phi_g - \Sigma_a^g \phi_g + \sum_{g'} \Sigma_s^{g' \to g} \phi_{g'} + \\ \qquad + (1-\beta) \chi_p^g \sum_{g'} \nu \Sigma_f^{g'} \phi_{g'} + \sum_j \chi_j^g \lambda_j C_j & g = 1, \ldots, N \\ \frac{\partial C_j(\mathbf{r},t)}{\partial t} = -\lambda_j C_j + \beta_j \sum_{g'} \nu \Sigma_f^{g'} \phi_{g'} & j = 1, \ldots, M \end{cases} \tag{18}$$

The exact boundary condition is given on the momentary boundary S_M by

$$\left. \frac{\partial \phi_g(\mathbf{r},t)}{\partial n} \right|_{\mathbf{r}_M} = -\frac{1}{l_g} \phi_g(\mathbf{r}_M, t) \tag{19}$$

The total energy spectrum χ^g, is related to the prompt and delayed spectra as

$$\chi^g = (1-\beta) \chi_p^g + \sum_j \beta_j \chi_j^g \tag{20}$$

As before, one derives a simplified boundary condition on the stationary boundary for each group g as

$$\left. \frac{\partial \phi_g(\mathbf{r},t)}{\partial n} \right|_{\mathbf{r}_B} \approx -\frac{1}{l_g} \phi_g(\mathbf{r}_B, t) + \frac{1}{l_g^2} \phi_g(\mathbf{r}_B, t) \varepsilon(\mathbf{r}_B, t) \tag{21}$$

Likewise in the one-group model, we additionally benefit from the simplified boundary condition (21) by defining the time-dependent group fluxes $\phi_g(\mathbf{r},t)$ over the static volume V_0.

3.2 LINEARISED EQUATIONS

Essentially in the same way as before one derives linearised multi-group equations, i.e. one splits time-dependent quantities into stationary components and small deviations. Next, one puts the splitting into the time-dependent equations (18) and takes into consideration the steady-state equations (16). This leads in the end to

$$\begin{cases} \dfrac{1}{\mathrm{v}_g}\dfrac{\partial \delta\phi_g(\mathbf{r},t)}{\partial t} = \nabla\cdot D^g\nabla\delta\phi_g - \Sigma_a^g\delta\phi_g + \sum\limits_{g'}\Sigma_s^{g'\to g}\delta\phi_{g'} + \\ \qquad\qquad +(1-\beta)\chi_p^g\sum\limits_{g'}\nu\Sigma_f^{g'}\delta\phi_{g'} + \sum\limits_j \chi_j^g\lambda_j\delta C_j \\ \dfrac{\partial \delta C_j(\mathbf{r},t)}{\partial t} = -\lambda_j\delta C_j + \beta_j\sum\limits_{g'}\nu\Sigma_f^{g'}\delta\phi_{g'} \end{cases} \tag{22}$$

No linearisation has been made so far. It is only the boundary condition that needs to be linearised. It becomes

$$\left.\frac{\partial \delta\phi_g(\mathbf{r},t)}{\partial n}\right|_{\mathbf{r}_B} = -\frac{1}{l_g}\delta\phi_g\left(\mathbf{r}_B,t\right) + \frac{1}{l_g^2}\phi_{0,g}\left(\mathbf{r}_B\right)\varepsilon\left(\mathbf{r}_B,t\right) \tag{23}$$

3.3 FREQUENCY-DEPENDENT EQUATIONS

Now it is easy to apply the Fourier transform to the linearised model to obtain equations in the frequency domain

$$\nabla\cdot D^g\nabla\delta\phi_g - (\Sigma_a^g + \frac{i\omega}{\mathrm{v}_g})\delta\phi_g + \sum_{g'}\Sigma_s^{g'\to g}\delta\phi_{g'} + \mathrm{X}^g(\omega)\cdot\sum_{g'}\nu\Sigma_f^{g'}\delta\phi_{g'} = 0 \tag{24}$$

Here, $\delta\phi_g$ are frequency-dependent and the new symbol, $\mathrm{X}^g(\omega)$, is introduced as follows

$$\mathrm{X}^g(\omega) \equiv (1-\beta)\chi_p^g + \sum_j \chi_j^g\beta_j\frac{\lambda_j}{\lambda_j+i\omega} = \chi^g - i\omega\sum_j\chi_j^g\frac{\beta_j}{\lambda_j+i\omega} \tag{25}$$

where χ^g is defined in (20). This allows us to rewrite equations (24) in a compact form as

$$\begin{cases} \nabla\cdot D^g\nabla\delta\phi_g + \sum\limits_{g'}S^{g'\to g}(\omega)\delta\phi_{g'} = 0 \\ \left.\dfrac{\partial \delta\phi_g(\mathbf{r},\omega)}{\partial n}\right|_{\mathbf{r}_B} = -\dfrac{1}{l_g}\delta\phi_g\left(\mathbf{r}_B,\omega\right) + \dfrac{1}{l_g^2}\phi_{0,g}\left(\mathbf{r}_B\right)\varepsilon\left(\mathbf{r}_B,\omega\right) \end{cases} \tag{26}$$

Eq. (26) is a multi-group analogue for (6). In addition, a short-cut notation was introduced as follows

$$S^{g'\to g}(\omega) \equiv -(\Sigma_a^g + \frac{i\omega}{\mathrm{v}_g})\delta_g^{g'} + \Sigma_s^{g'\to g} + \mathrm{X}^g(\omega)\cdot\nu\Sigma_f^{g'} \tag{27}$$

Here, $\delta_g^{g'}$ refers to the Kronecker delta function.

3.4 FULL SOLUTION IN FREQUENCY DOMAIN

Equation (26) can be solved by the Green's function method essentially in the same manner as before. First, we define the Green's function, $G(\mathbf{r}',g',\mathbf{r},g;\omega) \equiv G_{g',g}(\mathbf{r}',\mathbf{r};\omega) \equiv G_{g',g}$, as a solution to the system of N^2 equations

$$\begin{cases} \nabla \cdot D^g \nabla G_{g',g} + \sum_j S^{g\to j} G_{g',j} = \delta_g^{g'} \cdot \delta(\mathbf{r}-\mathbf{r}') \\ \left.\dfrac{\partial G_{g',g}}{\partial n}\right|_{\mathbf{r}_B} = -\dfrac{1}{l_g} G_{g',g} \qquad\qquad g,g' = 1,\ldots,N \end{cases} \tag{28}$$

Here $\delta(\mathbf{r}\text{-}\mathbf{r}')$ is the Dirac delta function. Second, we multiply the Green's function equations (28) by $\delta\phi_g$ and the neutron noise equations (26) by $G_{g',g}$, subtract each other and sum over energy groups. In the end this yields the solution as

$$\delta\phi_{g'}(\mathbf{r}',\omega) = -\int_{\partial V_0} \sum_g G(\mathbf{r}',g',\mathbf{r}_B,g;\omega) \frac{1}{l_g^2} D^g(\mathbf{r}_B)\phi_{0,g}(\mathbf{r}_B)\varepsilon(\mathbf{r}_B,\omega) dS(\mathbf{r}_B) \tag{29}$$

Eq. (29) is a direct generalisation of the one-group homogeneous representation (11) for the multi-group non-homogeneous model. We can cast solution (29) into a compact form by representing the Green's function $G(\mathbf{r}',g',\mathbf{r}_B,g;\omega)$ as a matrix Green's function, denoted as $\hat{\mathbf{G}}(\mathbf{r}',\mathbf{r};\omega)$, with the entries $G_{g',g}$ and using the ordinary vector-matrix notation with the following definitions

$$\delta\boldsymbol{\Phi} \equiv \begin{pmatrix} \delta\phi_1 \\ \vdots \\ \delta\phi_N \end{pmatrix};\ \boldsymbol{\Phi}_0 \equiv \begin{pmatrix} \phi_{0,1} \\ \vdots \\ \phi_{0,N} \end{pmatrix};\ \hat{\mathbf{l}} \equiv \begin{pmatrix} l_1 & & 0 \\ & \ddots & \\ 0 & & l_N \end{pmatrix};\ \hat{\mathbf{D}} \equiv \begin{pmatrix} D^1 & & 0 \\ & \ddots & \\ 0 & & D^N \end{pmatrix} \tag{30}$$

Then solution (29) takes the form

$$\delta\boldsymbol{\Phi}(\mathbf{r}',\omega) = -\int_{\partial V_0} \hat{\mathbf{G}}(\mathbf{r}',\mathbf{r}_B;\omega)\cdot\hat{\mathbf{l}}^{-2}\cdot\hat{\mathbf{D}}(\mathbf{r}_B)\cdot\boldsymbol{\Phi}_0(\mathbf{r}_B)\,\varepsilon(\mathbf{r}_B,\omega)\,dS(\mathbf{r}_B) \tag{31}$$

Eq. (29), or equivalently (31), represents the neutron noise $\delta\boldsymbol{\Phi}$ in terms of a linear integral operator acting on the noise source ε and entirely determined by the unperturbed system.

3.5 ABSORBER MODEL IN THE MULTI-GROUP CASE

The same argumentation as in the one-group case may be used to establish a multi-group version of the one-group absorber model. Omitting details we formulate here the final result. The fluctuating boundary is equivalent to placing an infinitely thin absorbing layer of varying strength onto the static surface:

$$\delta\Sigma_a^g(\mathbf{r},t) = -\frac{1}{l_g^2} D^g(\mathbf{r})\varepsilon(\mathbf{r},t)\delta\big(f(\mathbf{r})-c\big) \tag{32}$$

As was mentioned earlier, we suppose the static surface ∂V_0 be described through the equation $f(\mathbf{r})$=c.

3.6 KINETIC APPROXIMATIONS

Following [5] we start with the factorization principle as

$$\phi_g(\mathbf{r},t) = P(t)\psi_g(\mathbf{r},t) \tag{33}$$

In linear theory the normalisation condition can be given by integration over the static volume V_0 as

$$\frac{\partial}{\partial t}\int_{V_0}\sum_g \frac{1}{\mathrm{v}_g}\phi^+_{0,g}(\mathbf{r})\psi_g(\mathbf{r},t)dV = 0 \tag{34}$$

Here $\phi^+_{0,g}(\mathbf{r})$ refers to the adjoint function associated with the static critical system. If only the absorption cross section is perturbed, the reactivity term becomes [5]

$$\rho(t) = -\frac{1}{F(t)}\int_{V_0}\sum_g \phi^+_{0,g}(\mathbf{r})\delta\Sigma^g_a(\mathbf{r},t)\psi_g(\mathbf{r},t)dV \tag{35}$$

F(t) is usually given [5] as

$$F(t) = \int_{V_0}\sum_g\sum_{g'}\chi^g\nu\Sigma^{g'}_f(\mathbf{r})\phi^+_{0,g}(\mathbf{r})\psi_{g'}(\mathbf{r},t)dV \tag{36}$$

By using the absorber representation (32) we immediately obtain a general relationship, within the framework of linear theory, for the reactivity through the shape function and the noise source as

$$\rho(t) = +\frac{1}{F(t)}\int_{\partial V_0}\sum_g \phi^+_{0,g}(\mathbf{r}_B)\frac{1}{l_g^2}D^g(\mathbf{r}_B)\psi_g(\mathbf{r}_B,t)\,\varepsilon(\mathbf{r}_B,t)dS(\mathbf{r}_B) \tag{37}$$

The ordinary vector-matrix notation transforms (37) into a compact form of

$$\rho(t) = +\frac{1}{F(t)}\int_{\partial V_0}\boldsymbol{\Phi}^+_0(\mathbf{r}_B)\cdot\hat{\mathbf{l}}^{-2}\cdot\hat{\mathbf{D}}(\mathbf{r}_B)\cdot\boldsymbol{\Psi}(\mathbf{r}_B,t)\,\varepsilon(\mathbf{r}_B,t)\,dS(\mathbf{r}_B) \tag{38}$$

Here the adjoint fluxes $\phi^+_{0,g}$ are combined into a row-vector $\boldsymbol{\Phi}^+_0$. This immediately leads to different approximations of the reactivity term by assuming the point kinetic behavior, $\psi_g(\mathbf{r},t) = \phi_{0,g}(\mathbf{r})$, or the adiabatic behavior, $\psi_g(\mathbf{r},t) = \phi_{ad,g}(\mathbf{r},t)$.

4. ADJOINT FUNCTION REPRESENTATION

It is convenient to combine the group fluxes $\phi_1,\ldots,\phi_N$ into a column-vector $\boldsymbol{\Phi}$ of a direct space and the adjoint group fluxes $\psi^+_1,\ldots,\psi^+_N$ into a row-vector $\boldsymbol{\Psi}^+$ of an adjoint (dual) space. This allows us to use the ordinary vector-matrix notation, for instance, as follows

$$\boldsymbol{\Psi}^+ \equiv (\psi^+_1,\ldots,\psi^+_N);\quad \boldsymbol{\Phi} \equiv \begin{pmatrix}\phi_1\\ \vdots\\ \phi_N\end{pmatrix};\quad \boldsymbol{\Psi}^+\cdot\boldsymbol{\Phi} = \sum_g \psi^+_g\phi_g \tag{39}$$

The ordinary scalar product reads now as

$$\left(\boldsymbol{\Psi}^{+},\boldsymbol{\Phi}\right)=\int_{V_0}\boldsymbol{\Psi}^{+}(\mathbf{r})\cdot\boldsymbol{\Phi}(\mathbf{r})dV=\int_{V_0}\sum_{g}\psi_g^{+}(\mathbf{r})\phi_g(\mathbf{r})dV \tag{40}$$

Following the notations introduced in [7] one can write equations (26) in an operator form as

$$\hat{\mathbf{L}}(\mathbf{r},\omega)\equiv\nabla\cdot\hat{\mathbf{D}}(\mathbf{r})\nabla+\hat{\mathbf{S}}(\mathbf{r},\omega);\qquad\hat{\mathbf{L}}(\mathbf{r},\omega)\cdot\delta\boldsymbol{\Phi}=\delta\hat{\boldsymbol{\Sigma}}_a\cdot\boldsymbol{\Phi}_0\equiv\delta\mathbf{S} \tag{41}$$

The new symbol $\hat{\mathbf{S}}$ is a matrix with the entries $S^{g'\to g}$. In addition, the following definitions have been used

$$\delta\boldsymbol{\Phi}\equiv\begin{pmatrix}\delta\phi_1\\ \vdots\\ \delta\phi_N\end{pmatrix};\quad\delta\hat{\boldsymbol{\Sigma}}_a\equiv\begin{pmatrix}\delta\Sigma_a^1 & & 0\\ & \ddots & \\ 0 & & \delta\Sigma_a^N\end{pmatrix}\quad\boldsymbol{\Phi}_0\equiv\begin{pmatrix}\phi_{0,1}\\ \vdots\\ \phi_{0,N}\end{pmatrix} \tag{42}$$

It is convenient to define a left multiplication given in a component-wise manner as

$$\left(\boldsymbol{\Psi}^{+}\cdot\hat{\mathbf{L}}\right)_g\equiv\nabla\cdot D^g\nabla\Psi_g^{+}+\sum_{g'}S^{g\to g'}\Psi_{g'}^{+} \tag{43}$$

Then one can introduce the dynamic adjoint function as a solution to the equation

$$\boldsymbol{\Psi}^{+}(\mathbf{r},\mathbf{r}_0,\omega)\cdot\hat{\mathbf{L}}(\mathbf{r},\omega)=\boldsymbol{\Sigma}_d(\mathbf{r},\mathbf{r}_0,\omega)\equiv\left(\Sigma_d^1,\ldots,\Sigma_d^N\right) \tag{44}$$

It is customary to assume Σ_d^g be the group cross sections of a detector located at around the point $\mathbf{r}_0$. The left-right multiplication formalism readily gives the identity

$$\left(\boldsymbol{\Sigma}_d,\delta\boldsymbol{\Phi}\right)=\int_{V_0}\boldsymbol{\Psi}^{+}\cdot\hat{\mathbf{L}}\cdot\delta\boldsymbol{\Phi}\,dV=\left(\boldsymbol{\Psi}^{+},\delta\mathbf{S}\right) \tag{45}$$

Since in most practical cases detectors used in noise measurement are sensitive to thermal neutrons only, it is sufficient to calculate only the thermal noise. To be a bit more general we define a point-like g-detector (i.e. a detector sensitive to the neutrons of the energy group g only) as

$$\boldsymbol{\Sigma}_d^g(\mathbf{r},\mathbf{r}_0)\equiv\left[\Sigma_d^{g,1},\Sigma_d^{g,2},\ldots,\Sigma_d^{g,N}\right]=\left[0,\ldots,\delta(\mathbf{r}-\mathbf{r}_0),\ldots,0\right];\ \Sigma_d^{g,g'}=\delta(\mathbf{r}-\mathbf{r}_0)\,\delta_g^{g'} \tag{46}$$

In this case, the corresponding adjoint function, as a solution to (44) with the right hand side $\boldsymbol{\Sigma}_d^g(\mathbf{r},\mathbf{r}_0)$, becomes dependent on the parameter g and has components

$$\boldsymbol{\Psi}_g^{+}(\mathbf{r},\mathbf{r}_0,\omega)=\left[\psi_{g,1}^{+}(\mathbf{r},\mathbf{r}_0,\omega),\ldots,\psi_{g,N}^{+}(\mathbf{r},\mathbf{r}_0,\omega)\right] \tag{47}$$

By setting $\boldsymbol{\Psi}^{+}=\boldsymbol{\Psi}_g^{+}$ in (45) one easily obtains the representation of the neutron noise in the multi-group model as

$$\delta\phi_g(\mathbf{r}_0,\omega)=\left(\boldsymbol{\Psi}_g^{+},\delta\mathbf{S}\right)=\int_{V_0}\sum_{g'}\psi_{g,g'}^{+}(\mathbf{r},\mathbf{r}_0,\omega)\delta\Sigma_a^{g'}(\mathbf{r},\omega)\phi_{0,g'}(\mathbf{r})dV(\mathbf{r}) \tag{48}$$

Eq. (48) shows a certain advantage of the adjoint function approach over the Green's function method if one needs exclusively the noise in one group. In this case the Green's function technique requires knowledge of the N^2 components $G_{g',g}(\mathbf{r}',\mathbf{r};\omega)$ in contrast to the N components $\psi_{g,g'}^{+}(\mathbf{r},\mathbf{r}_0,\omega)$. The absorber model (32) immediately transforms (48) to the following expression

of the neutron noise induced by vibrating boundaries

$$\delta\phi_g(\mathbf{r}_0,\omega) = \int_{\partial V_0} \sum_{g'} \psi^+_{g,g'}(\mathbf{r}_B,\mathbf{r}_0,\omega)\frac{1}{l^2_{g'}} D^{g'}(\mathbf{r}_B)\phi_{0,g'}(\mathbf{r}_B)\varepsilon(\mathbf{r}_B,\omega)dS(\mathbf{r}_B) \tag{49}$$

Once again one casts (49) into a compact form by using the diagonal matrices $\hat{\mathbf{l}}$ and $\hat{\mathbf{D}}$ defined in (30). Then (49) becomes

$$\delta\phi_g(\mathbf{r}_0,\omega) = \int_{\partial V_0} \boldsymbol{\Psi}^+_g(\mathbf{r}_B,\mathbf{r}_0,\omega)\cdot\hat{\mathbf{l}}^{-2}\cdot\hat{\mathbf{D}}(\mathbf{r}_B)\cdot\boldsymbol{\Phi}_0(\mathbf{r}_B)\,\varepsilon(\mathbf{r}_B,\omega)\,dS(\mathbf{r}_B) \tag{50}$$

Here again, we can state that solution (50) gives a representation of the neutron noise at a detector location in terms of a linear integral operator belonging to the static system and the noise source.

5. IN-CORE NOISE INDUCED BY BOUNDARY VIBRATIONS

5.1 CORE BARREL MOVEMENTS AND EX-CORE NOISE

Core barrels of PWRs have long been known to undergo both pendulum-like (beam mode) and shape distorting (shell mode) vibrations. Analysis of these vibrations has traditionally been based on the use of ex-core detector signals. Monitoring of the vibrations by means of neutron sensors is an important practical problem. Changing characteristics of the vibrations might indicate deteriorating material properties, as was shown at a quite early stage of reactor diagnostics in the case of the German STADE power plant [8].

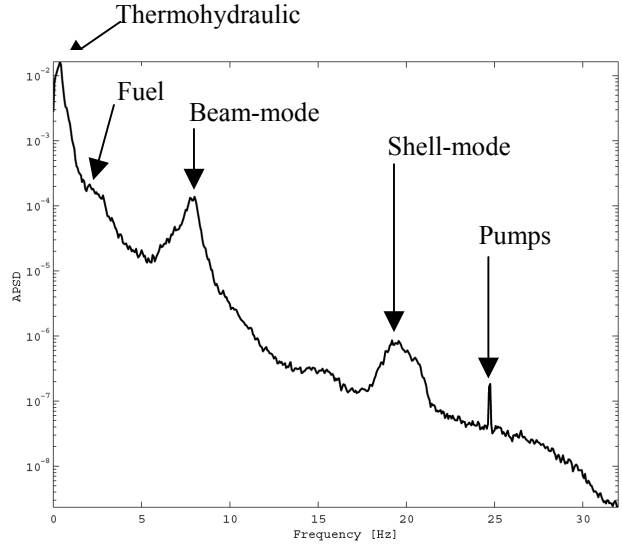

- Thermohydraulic fluctuations 0.1 – 1 Hz
- Collective fuel vibrations 2 – 5 Hz
- Core barrel beam mode 8 Hz
- Core barrel shell mode 20 Hz
- Main coolant pumps 25 Hz

Figure 2. Typical power spectrum of ex-core signal

Whereas the diagnostics of beam mode vibrations is generally considered as working satisfactorily by ex-core ionisation chambers, a special difficulty arises concerning the diagnostics of shell-mode vibrations in 4-loop Westinghouse type PWRs. The reason is that in those plants, at one axial level there are four ex-core detectors with a spacing of 90°. Due to the special symmetry of the ex-core noise induced by shell vibrations, in such a case all four detector signals are equivalent. This single measured quantity is not sufficient to unfold two unknowns, namely the vibration amplitude and the direction of vibrations. In addition, in special cases (vibration axes 45° to the detector lines) the vibrations may not be detected at all.

To remedy this situation we suggest that in addition to the ex-core noise, also the in-core noise, induced by the distortion of the core shape ("fluctuating boundary") or, equivalently, the motion of the core barrel relative to the pressure vessel, is also used. This suggestion is based on the recent recognition that core-barrel vibrations also induce in-core noise [9]. Use of the in-core noise would enhance the possibilities of diagnostics, because in most PWR cores, there are a large number of in-core detector positions available in the core.

5.2 MODEL OF CORE BARREL MOTION

To apply the general method for core barrel vibrations, one needs to find a suitable representation of the function $\varepsilon(\mathbf{r}_B,\omega)$ that describes the variations of the boundary. This is relatively straightforward if we consider small vibrations of an incompressible core, which is cylindrical in the non-perturbed case. Denoting the momentary boundary of the core as

$$R(\varphi,t) = R_0 + \varepsilon(\varphi,t) \tag{51}$$

where R_0 is the static radius, then the function $\varepsilon(\varphi,t)$ can be expanded into a trigonometric series as

$$\varepsilon(\varphi,t) = \sum_{n=1}^{2}\left[a_n(t)\cdot\cos n\varphi + b_n(t)\cdot\sin n\varphi\right] \equiv \sum_{n=1}^{2}\varepsilon_n(\varphi,t) \tag{52}$$

Mode 0 is absent due to the incompressibility assumption, and the higher modes are assumed to be negligible. Mode 1 describes the pendulum-like or beam mode vibrations, whereas mode 2 refers to the shell mode motion. The functions $a_n(t)$ and $b_n(t)$ may be interpreted as stochastic processes because in practice $\varepsilon(\varphi,t)$ is only determined in a statistical sense. Since the eigenfrequencies of the different vibration modes are different, in the frequency domain analysis we can separate these two components. Their treatment and the applied diagnostic procedures will also be somewhat different.

The beam mode vibrations are considered as a two-dimensional random walk and are described by the correlation properties between the coefficients $a_1(t)$ and $b_1(t)$. Such a motion has usually a non-isotropic 2D distribution, which is quantified by the so-called $k-\alpha$ model, through an anisotropy factor and the preferred direction of vibrations [2]. Determination of k and α has been achieved successfully by ex-core detectors in the past, thus this problem will not be investigated in this paper. The shell mode vibrations are assumed to have the main axes of vibration fixed. Thus it is convenient to cast this mode into an amplitude and phase representation, which in the frequency domain reads as

$$\varepsilon_2(\varphi,\omega) = a_2(\omega)\cdot\cos 2\varphi + b_2(\omega)\cdot\sin 2\varphi = \delta R_2(\omega)\cos 2(\varphi-\chi) \tag{53}$$

5.2 FULL SOLUTION FOR CYLINDRICAL CORE BARREL

To analyze practical cases we restrict ourselves to the one-speed homogeneous model. The solution for a cylindrical core barrel may be obtained either by expanding the Green's function into a series of eigenfunctions or by applying directly the variable separation method. Taking into account (52) this leads to

$$\begin{aligned}\delta\phi(r,\varphi;\omega) &= \frac{\phi_0(R_0)}{l}\sum_{n=1}^{2}\frac{J_n\left(B(\omega)r\right)}{lB(\omega)J_n'\left(B(\omega)R_0\right)+J_n\left(B(\omega)R_0\right)}\varepsilon_n(\varphi;\omega) \equiv \\ &\equiv \delta\phi_1(r,\varphi;\omega)+\delta\phi_2(r,\varphi;\omega)\end{aligned} \tag{54}$$

Here, J_n is the Bessel function of the first kind. Representation (54) defines modal transfer functions

$\delta\phi_n(r,\varphi;\omega) \equiv G_n(r,\omega)\cdot\varepsilon_n(\varphi;\omega)$ as

$$G_n(r,\omega) = \frac{\phi_0(R_0)}{l}\frac{J_n\left(B(\omega)r\right)}{lB(\omega)J_n'\left(B(\omega)R_0\right)+J_n\left(B(\omega)R_0\right)} \tag{55}$$

The auto power spectral density (APSD) of the beam (*n=1*) and shell (*n=2*) mode components is then given, through the Wiener-Khinchin theorem, as

$$APSD_n(r,\varphi;\omega) = \left|G_n(r,\omega)\right|^2\ APSD_{\varepsilon,n}(\varphi;\omega) \tag{56}$$

5.3 ANALYSIS OF THE SOLUTION

Regarding the radial dependence of the in-core noise, as (54) and (56) show, the noise amplitude is zero in the middle of the core for both perturbations (beam and shell mode), and increases monotonically towards the boundary along any given radial direction. This is because the perturbation is situated at the core boundary, at the noise decreases away from the perturbation. This suggests that in-core detectors close to the boundary should be used since detectors in the central core regions are of very little use; indeed, this conclusion is confirmed by the measurements, as will be seen below.

An analysis of eqn (54) together with (52) shows that for both the beam mode and the shell mode, the azimuthal dependence of the in-core noise is the same as that of the ex-core detectors. For instance, detectors in diagonally opposite positions will have opposite phase for pendular vibrations, whereas they will be in-phase for shell mode vibrations. Such relationships can for instance help in estimating the direction of vibrations for shell mode vibrations in an empirical way. The formulas of course will make it possible to elaborate algorithmic determination of the vibration axes as well.

Regarding the azimuthal distribution of the noise amplitude, there is a difference between the two modes. Because of the mentioned nearly isotropic 2-D random walk character of the pendular motion, the APSD of $\varepsilon_1(\varphi;\omega)$ will show only a weak azimuthal dependence. This is because the motion is not unidirectional. For the shell-mode vibrations, however, the vibration angle χ can be assumed constant, and the azimuthal dependence of the noise amplitude is described by

$$\begin{aligned} &APSD_2(r,\varphi;\omega) = \left|G_2(r,\omega)\right|^2\cos^2 2(\varphi-\chi)\cdot APSD_{\delta R}(\omega) \equiv \\ &\equiv A(r,\omega)\left[1+\cos 4(\varphi-\chi)\right]\cdot APSD_{\delta R}(\omega) \equiv A_2(r,\varphi;\omega)\cdot APSD_{\delta R}(\omega) \end{aligned} \tag{57}$$

Representation (57) shows a remarkable fact: the radial and angular variables are separated. In addition, it enables us to define a shell mode transfer function, *$A_2(r;\varphi;\omega)$*, as

$$A_2(r,\varphi;\omega) = \frac{1}{2}\left|\frac{\phi_0(R_0)}{l}\frac{J_2\left(B(\omega)r\right)}{lB(\omega)J_2'\left(B(\omega)R_0\right)+J_2\left(B(\omega)R_0\right)}\right|^2\left[1+\cos 4(\varphi-\chi)\right] \tag{58}$$

This transfer function for the shell mode vibrations, *$A_2(r;\varphi;\omega)$*, is shown in Figure 3. Thus the azimuthal dependence of the noise amplitude will show four maxima along the two major axes of vibrations, and four minima along the two perpendicular nodal lines that are to 45º to the vibration axes. As it will be shown, this dependence can be discerned from the measurements.

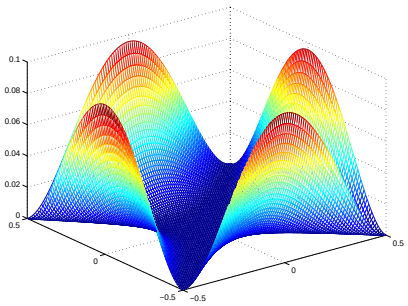

Figure 3. Transfer function for the shell mode

5.4 DETERMINATION OF THE VIBRATIONAL ANGLE

From the formulae above, algorithmic relationships, based on the signal auto- and cross-spectra, can also be derived for the unfolding of the vibration parameters from the measured signals. Here we only will show one of them, the determination of the vibration angle for the shell-mode. Assume we know $APSD_2$ values for two different detectors situated at, say, (r_1,φ_1) and (r_2,φ_2), as shown in Figure 4. Then the representation (57) allows us to set up an equation with respect to χ by dividing one value by the other:

$$a^2 \equiv \frac{APSD_2(r_2,\varphi_2;\omega)}{APSD_2(r_1,\varphi_1;\omega)} = \frac{\left|J_2\left(B(\omega)r_2\right)\right|^2 \cos^2 2(\varphi_2-\chi)}{\left|J_2\left(B(\omega)r_1\right)\right|^2 \cos^2 2(\varphi_1-\chi)} \tag{59}$$

The solution is given by

$$\chi = \frac{1}{2}\arctan\frac{\left|J_2\left(B(\omega)r_1\right)\right|\cos 2\varphi_2 - a\left|J_2\left(B(\omega)r_2\right)\right|\cos 2\varphi_1}{\left|J_2\left(B(\omega)r_1\right)\right|\sin 2\varphi_2 - a\left|J_2\left(B(\omega)r_2\right)\right|\sin 2\varphi_1} \tag{60}$$

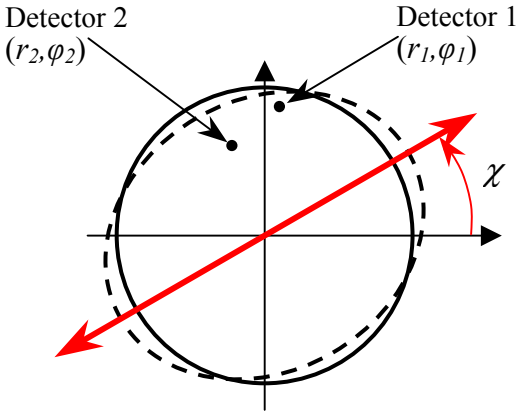

Figure 4. Determination of the vibration axis by two detectors.

However, application of such formulas is significantly more complicated than the simple phase relationships described above. The main reason is that, unlike the phase relationships that are based on cross correlation from which the uncorrelated background will drop out, eqn (60) is based on the APSDs with a large background (see Figure 6). Due to this and other reasons, no application of the

algorithmic unfolding methods will be reported in this paper.

Another possibility to uncover the vibration angle also follows from the solution structure of the shell mode

$$\delta\phi_2(r,\varphi;\omega) = \frac{\phi_0(R_0)}{l}\frac{J_2\left(B(\omega)r\right)}{lB(\omega)J_2'\left(B(\omega)R_0\right)+J_2\left(B(\omega)R_0\right)}\cos 2(\varphi-\chi)\delta R_2(\omega) \qquad (61)$$

Assume we are lucky to find two detectors, which are angularly close to each other on the one hand, and which are out of phase on the other hand. Then we can draw one of the nodal lines somewhere in between the two detectors as shown in Figure 5. This readily gives the other nodal line as perpendicular to the first one. Finally, we obtain the axes of the shell mode by drawing the bisectors shown in Figure 5 with the two-headed arrow.

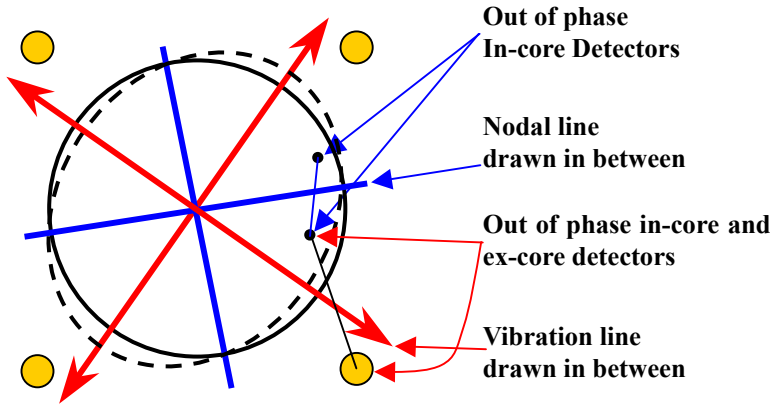

Figure 5. Phase analysis for the shell mode

The phase relationships between in-core and ex-core detectors are somewhat more complicated. On the first sight they would follow the same pattern as within the group of ex-core or in-core detectors. A closer examination shows, however, these cross-relationships between one in-core and one ex-core detector contain an extra additional factor of 180°, i.e. all phase relationships are reversed compared to the intra-group (pure in-core or pure ex-core) phases. The reason for this is that in contrast to the simple model of a bare core used in the foregoing, the real core is a reflected one. The consequence of this is that the formulas derived for the in-core noise as induced by the fluctuation of the boundary need to be taken with an opposite sign when describing the vibration of the core in a static reflector. An outward motion of the core boundary in a bare system leads to flux increase in its neighbourhood, and to flux decrease in a reflected system, due to decreasing reflector thickness. Because of this, if we find one in-core and one ex-core detector angularly close to each other, which exhibit out of phase behaviuor, then we can draw the vibration line somewhere in between as shown in Figure 5. The validity of this assumption will be further analysed in future model calculations and experiments.

5.5 DESCRIPTION OF IN-CORE MEASUREMENTS

A number of measurements to evaluate in-core noise were taken in 1994 at the Swedish nuclear power plant Ringhals, Unit 3. Each measurement involves 5 movable in-core detectors and a sampling frequency of 64 Hz. Measurement time is about 17 minutes, which results in more than 65000 samples. Figure 6 below shows the core cross-section of the core together with the five detector positions. It should be stressed here that originally the experiments were designed for a completely different purpose that resulted in the detector layout being far from optimal.

A typical measurement result is shown in Figure 6, which displaying the APSD of two in-core detectors, as well as the coherence and phase between them. As described in the earlier publications [2], the peak at 8 Hz corresponds to the beam mode, whereas the other peak at 20 Hz is due to the shell mode vibrations. These peaks are much smaller than those observed in the ex-core detector signals, (see Figure 2), especially for the shell mode. As seen in Figure 6, some of the peaks at 20 Hz can hardly be observed. In contrast to that, the coherence, while being relatively low, is still quite visible. The figure clearly shows the difficulties of unfolding methods using the quantitative values of the APSDs. The area below each peak, after separation from the background, was determined by an algorithm and will be called Area1 and Area2 in the continuation. The phase relationships, on the other hand, can be used more flexibly.

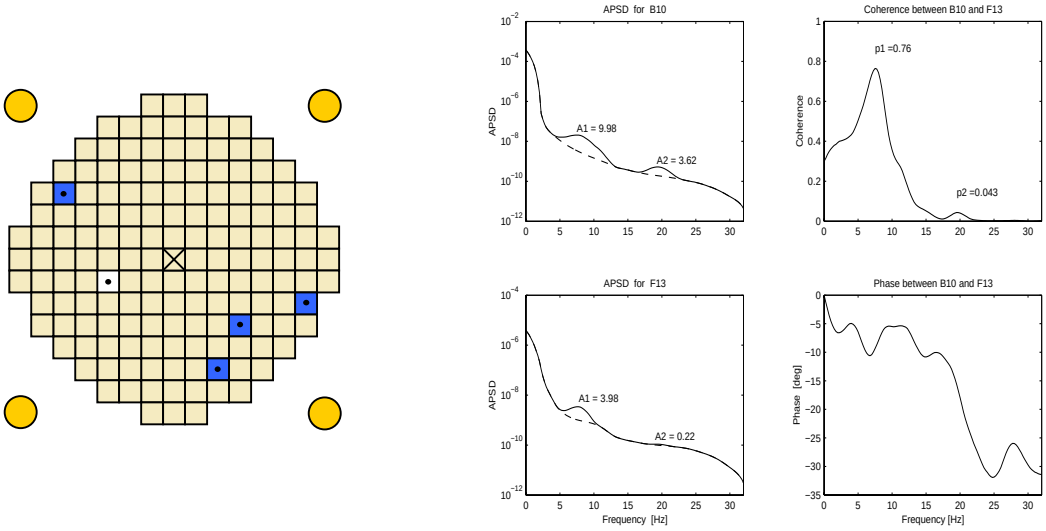

Figure 6. Experimental layout and typical power spectra

5.6 CORRELATION BETWEEN IN-CORE AND EX-CORE DETECTORS

While analyzing the experimental data we have found somewhat contradictory behaviour of in-core and ex-core detectors. Namely, assume an in-core and an ex-core detector lie in the same nodal quadrant as shown in Figure 5. Our simple model (61) would suggest an in-phase correlation of these detectors. Many measurements, however, were not consistent with this theoretical conclusion. The fact can have several reasons. One thing is that, even the ex-core measurements are not seldom giving some contradictory phase relationships, although the theory of ex-core noise induced by core-barrel vibrations is quite straightforward and generally accepted. The reason could be strong background noise, simultaneous presence of some other noise source at the same frequency.

As was already discussed in section 5.4, a more relevant reason might be the fact that the physical model of shell-mode vibrations may not correspond well to the real vibrations. It is easy to confirm that the model of perturbation (shell mode vibrations) used as a source of the in-core noise is valid for either pure core-barrel vibrations with a stationary pressure vessel, or with a vibrating pressure vessel with a stationary core (see Figure 7).

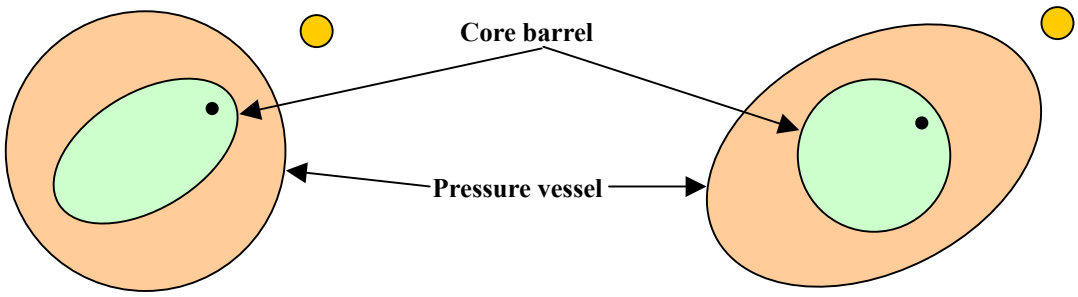

Figure 7. Two different cases of core-barrel vibrations

Nevertheless, in the both cases, the in-phase and out-of-phase relationships between in-core and out-of-core detectors are opposite to those in the first case. In other words, in-core and ex-core detectors in the same quadrant would have out-of-phase behaviour. In reality, both types shown in Figure **7** can occur simultaneously, correlated or uncorrelated with each other. Another possibility is that, unlike it was assumed in the present study, the vibration direction is not constant. Formally, this would mean that both $a_2(t)$ and $b_2(t)$ are non-zero stochastic processes that can be defined through their auto- and cross-spectra. The theory used in the present study is not valid for any of these cases. The character of ex-core noise, on the other hand, is not so sensitive for such complications of the vibration pattern.

5.7 EVALUATION OF VIBRATIONAL AXES

An experimental layout and a qualitative description of measurements are visually given in Figure 8.

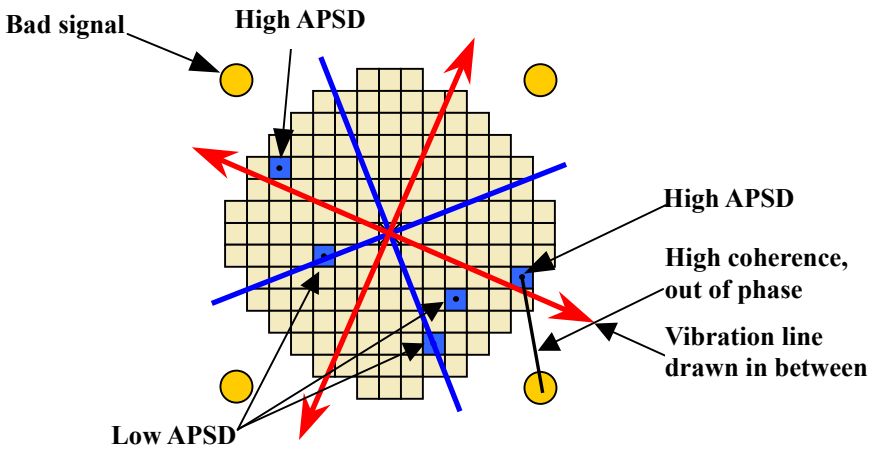

Figure 8. Evaluation of the vibration axis

To evaluate the vibration direction we take into consideration the following facts:

- Two almost opposite in-core detectors, which are close to the boundary, show high APSD;
- One of these detectors is out of phase with the nearest ex-core detector;
- The other in-core detectors give low APSD.

To match the above information we draw the vibration axes as shown in Figure 8. It would be helpful to have more in-core detectors. For example, one of the vibration axes has no in-core detectors in its vicinity. Such a detector could give a strong evidence for or against the theoretical model.

CONCLUSIONS

Generally speaking, the principal purpose of neutron noise theory is to relate the neutron noise $\delta\phi$ to the noise source $\delta\varepsilon$ through a certain operator $\hat{\mathbf{G}}$, which is traditionally called the transfer function. Symbolically this can be written as

$$\delta\phi = \hat{\mathbf{G}} \cdot \delta\varepsilon$$

The notion becomes of particular importance if we are able to meet the conditions:

- $\hat{\mathbf{G}}$ is entirely determined by the unperturbed system;
- $\hat{\mathbf{G}}$ is a linear operator.

The present work gives such a representation of the in-core neutron noise caused by small boundary movements for the general non-homogeneous problem in the multi-group diffusion approximation. The absorber model is then proposed, since it turns out to be very useful, for example, in deriving the point reactor and adiabatic approximations of the neutron noise arising from fluctuating boundaries.

The analysis of the measurements supports the validity of the theory of in-core noise, induced by core barrel vibrations. Some diagnostic conclusions could also be drawn. For the 8 Hz peak in the in-core spectra, it was found that it is most likely induced by the pendular vibrations of the core barrel, as opposed to the earlier suggestion that it arises from individual vibrations of fuel assemblies, induced by the pendular vibrations. For the shell-mode vibrations, a guess for the direction of the vibrations could be given. This was not possible before, when only the ex-core detector signals were used, since they have a disadvantageous positioning around the vessel.

In order that the diagnostic use of the in-core noise be effective, a relatively large amount of in-core detectors is necessary, more that what was available in the present analysis. Further, positioning of these detectors is important; they should be close to the core periphery and restricted into one quadrant of the core if there are only a few detectors. With proper arrangement of in-core detectors the in-core noise could enhance the possibilities of core-barrel vibration diagnostics.

ACKNOWLEDGEMENTS

This project was supported by the Swedish Nuclear Power Inspectorate, contract 14.5-011132-01225.

REFERENCES

1. N. S. Garis, I. Pázsit, and D. C. Sahni, "Modelling of a Vibrating Reactor Boundary and Calculation of the Induced Neutron Noise," *Annals of Nuclear Energy*, **23**, pp.1197-1208 (1996).
2. I. Pázsit , J. Karlsson, N. S. Garis, "Some Developments in Core-Barrel Vibration Diagnostics," *Annals of Nuclear Energy*, **25**, pp.1079-1093 (1998).
3. D. C. Sahni, I. Pázsit, and N. S. Garis, "A Transformation Technique to Treat Strong Vibrating Absorbers," *Annals of Nuclear Energy*, **26**, pp.1551-1567 (1999).
4. I. Pázsit , V. Arzhanov, "Linear Reactor Kinetics and Neutron Noise in Systems with Fluctuating Boundaries," *Annals of Nuclear Energy*, **27**, pp.1385-1398 (2000).
5. G. E. Bell, S. Glasstone, *Nuclear Reactor Theory*, Van Nostrand-Reinhold, New York (1970).
6. V. Arzhanov, "Multi-Group Theory of Neutron Noise Induced by Vibrating Boundaries," *Annals of Nuclear Energy*, **29/18**, pp.2143-2158 (2002).
7. I. Pázsit, "Dynamic Transfer Function Calculations for Core Diagnostics," *Annals of Nuclear Energy*, **19, No 5**, pp.303-312 (1992).
8. V. Bauernfeind, *Progress in Nuclear Energy*, **1**, pp.323-332 (1977).
9. C. Demazière, V. Arzhanov, and I. Pázsit "Ringhals Diagnostics and Monitoring. Stage 6," Chalmers/Ringhals Report CTH-RF-161/RR-8 (2001).